J Solid State Electrochem (2012) 16:3371–3381
DOI 10.1007/s10008-012-1781-9

ORIGINAL PAPER

Towards the mechanism of Li^+ ion transfer in the net solid polymer electrolyte based on polyethylene glycol diacrylate–$LiClO_4$

O. V. Yarmolenko · K. G. Khatmullina · G. Z. Tulibaeva · L. M. Bogdanova · A. F. Shestakov

Received: 1 August 2011 / Revised: 14 May 2012 / Accepted: 18 May 2012 / Published online: 6 June 2012

Abstract Ion transport in the new three-dimensional network polymer electrolytes that are completely amorphous in the solid state has been studied on the example of the matrix model with a monomer—polyethylene glycol diacrylate, cross-linked by radical polymerization. The nature of ionic conductivity in solid polymer electrolytes based on polyethylene glycol diacrylate at different concentrations of salt $LiClO_4$ was studied by methods of electrochemical impedance, differential scanning calorimetry analysis, Fourier transform infrared spectroscopy and quantum chemical modeling. The maximum value of conductivity in the range of 20–100 °C is realized at 20 wt% content of $LiClO_4$. The reason for the low conductivity of the SPE studied is the small degree of dissociation of contact ion pairs. At the increase in the salt content associates of contact pairs $Li^+ClO_4^-$, dimers and trimers (at $LiClO_4$ >20 wt%) are formed. The appearances of trimers are accompanied by a decrease in conductivity due to lowering of contact pair content.

Keywords Polymer electrolyte · Li^+ ion · $LiClO_4$ salt · Ion pair · Polyethylene glycol diacrylate · Conductivity · Quantum-chemical modeling · FTIR spectra

Introduction

The first solid polymer electrolyte (SPE) for lithium power sources was proposed by Armand et al. in 1978 [1]. High-molecular polyethylene oxide (PEO), $–(C_2H_4O)_n–$, with a molecular weight of 500,000, was investigated as the polymer matrix. With subsequent study of this system, it was found that the maximum conductivity is achieved at the composition of $(C_2H_4O)_8LiClO_4$, i.e., one Li^+ ion on a fragment of the polymer chain with eight oxygen atoms. A hopping conduction mechanism with a Li^+ ion movement between equilibrium positions was assumed.

The low conductivity of the solid electrolyte based on high-molecular PEO and $LiClO_4$ salt of the order of 10^{-8} S× cm^{-1} [1] at room temperature is caused by the high degree of crystallinity of the polymer matrix. It has been found using ^7Li NMR spectroscopy that the cation transport in the electrolyte occurs predominantly in amorphous regions, and in the crystalline regions, its motion is almost frozen.

The large number of the works was dedicated to selection of the polymer matrix for SPE. As a result of these studies, sufficiently strong requirements for polymers were formulated, which can be used as part of SPE in lithium power sources [2, 3]:

- The structure of the main or side polymer chain has to contain heteroatoms with high basicity, capable to solvate Li^+ ions that led to the salt dissociation.
- Heteroatoms in the polymer chain should be placed at the periodicity that would promote the fast transport of Li^+ ions.
- Polymer should not be crystalline and should have a glass transition temperature below the operating temperature of the power source to promote the fast Li^+ transport.
- Polymer should be chemically and electrochemically stable with respect to electrode materials, as well as it should possess the ability to form mechanically strong films for the assembly of chemical power source.

In this connection, there arises a particular interest to the net polymer electrolytes, which are completely amorphous.

O. V. Yarmolenko · K. G. Khatmullina · G. Z. Tulibaeva (✉) · L. M. Bogdanova · A. F. Shestakov
Institute of Problems of Chemical Physics of the Russian Academy of Sciences, Semenov av., 1, Chernogolovka, Moscow Region 142432, Russian Federation
e-mail: tulibaeva@gmail.com

Net polymer electrolytes [4, 5] are formed by connection of the terminal C=C groups under the influence of photo- or thermo-initiator by a radical mechanism. Thus, a three-dimensional network structure is formed, which is difficult to represent in two dimensions (see the scheme shown below):

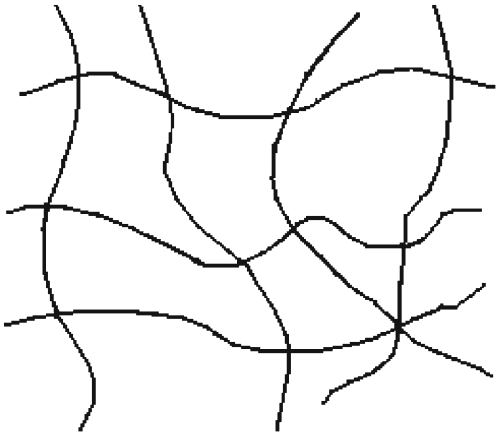

Usually, the molecular weight of network polymers is more than 10^9 g/mol, i.e., the whole volume the polymer is comparable with the size of a single molecule.

The most important advantage of the matrix based on polyether or polyester diacrylates is their complete amorphousness. The formation of the crystalline phase, as is the case in linear polymers such as polyethylene oxide, is practically impossible due to the statistic nature of three-dimensional cross-linking. Therefore, such network structures attract much attention in terms of possible application for solid electrolyte design.

There is a whole direction in the development of polymer electrolytes by radical polymerization of polyester and polyether diacrylates [6–13]. Among them, polyethylene glycol diacrylate (PEG-DA), which contains ethylene oxide units, is of special interest. To date, a whole number of works on synthesis and study of polymer electrolytes based on PEG-DA appeared (see for example [14, 15]). However, for the directed synthesis of polymer electrolytes for lithium-polymer batteries with improved characteristics, it is necessary to study the mechanism of Li^+ ions transport in such systems. Such investigations are not so much presented now [16, 17].

Previously, we studied polymer gel electrolytes based on different polyester and polyether diacrylates for lithium power sources [18–21] and found that the highest conductivity of the electrolytes achieved is comparable with that of the liquid phase at the concentration of lithium ion about 1 mol/dm^3. However, in solid polymer systems without a solvent, this salt concentration is not enough to realize the maximal value of the conductivity [22].

A feature of the net matrix based on polyester or polyether diacrylate is that, near the knocks of net, there are carbonyl C=O groups with potential high affinity to a lithium ions, which could serve as traps for Li^+ ions.

This paper is devoted to the analysis of the molecular structure of the polymer electrolyte based on PEG-DA with different $LiClO_4$ contents using obtained experimental data on the conductivity, Fourier transform infrared (FTIR) spectroscopy, and the results of quantum-chemical modeling in order to determine more favorable coordination sites for lithium ion as well as to understand the influence of counter ion ClO_4^- on the Li^+ mobility.

A similar complex approach has been used in the works of Abbrant S. to investigate the conductivity of polymer gel electrolytes based on a cross-linked polyethylene oxide, nano(ethylene oxide)dimethacrylate, and fluorinated copolymer, polyvinylidene fluoride-hexafluoropropylene [23], or oligo(ethylene glycol) dimethacrylate [24] in the presence of solvents: propylene carbonate and dimethyl sulfoxide.

Experimental

We used the following reagents.

Poly(ethylene glycol) diacrylate (PEG-DA) (“Aldrich”):

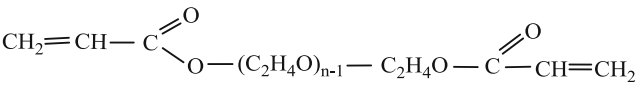

PEG-DA has the following characteristics: average molecular weight M_n=435, which corresponds to the average value n=7.5; melting point T_{melt}=−10 °C; glass transition temperature T_g=−73.5 °C; boiling point T_{boil}=104 °C; d_4^{20}=1.114–1.124; viscosity η^{25}=57 sP (25 °C); and C=C bonds concentration=4.6×10^{-3} mol/g.

$LiClO_4$ (Aldrin) was 99.99 % grade (T_{melt}=236 °C; T_{fl}=106 °C). Benzene peroxide (Aldrin) was purified by recrystallization from chloroform, then by drying at room temperature, first on the air, then in a vacuum.

Synthesis of solid polymer electrolyte

Samples of PEG-DA and $LiClO_4$ were stirred at 40–60 °C about 24 h until complete dissolution of the salt. Then, benzene peroxide (0.8 wt%) was added and dissolved at 40 °C (30–60 min). The mixture was evacuated for 15–30 min to remove air bubbles. The resulting homogeneous solution was poured to the preheated glass reactor, treated by dimensionality to prevent adhesion, and was solidified according stepwise heating regime: T_1=80 °C (5 h); T_2=140 °C (2 h). Thus, formed transparent films had thickness d=0.0082–0.0114 cm.

Electrochemical impedance spectroscopy method

Electrochemical impedance was measured in symmetrical cells with stainless steel (SS) electrodes (SS/SPE/SS) using an LCR measuring instrument from Goodwill Instrument Co. Ltd. in the frequency range of $12–1\times10^5$ Hz. The amplitude of the AC signal was 10 mV. Thermostat TG-TC-01 was used to study the temperature dependence of the bulk conductivity in the electrolyte.

Data obtained by electrochemical impedance spectroscopy of SS/SPE/SS cell were analyzed by the standard scheme:

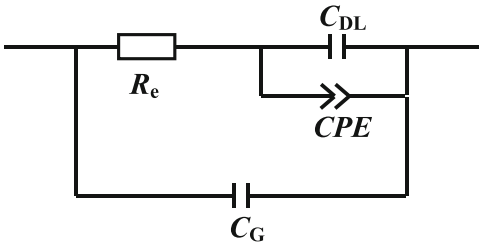

where R_e is the electrolyte resistance, C_G is the geometric capacity, C_{DL} is the double layer capacity, and CPE is the constant phase shift element. The C_{DL} and CPE elements characterize the electrode impedance: $Z_{CPE}=Aj\omega^{-P}$, $j=(-1)^{1/2}$. Equivalent circuit parameters were calculated using the program of ZView2. The calculated conductivities are presented in the Table 1.

The scheme provides a satisfactory description of the hodograph of SS/SPE/SS cells. Figure 1 shows a typical form of the hodograph for cells with SPE based on PEG-DA and $LiClO_4$.

The hodograph is a combination of a straight line with a slope of 60–65° and a part of the circular arc. The arc is most pronounced at low temperatures and goes to coordinate origin at extrapolation to higher frequencies. This type of frequency dependence characterizes the geometric capacity of the cell.

In this approach, the measured conductivity consists of two contributions: transfer of cations and transfer of anions. Usually in the SPE studied, the lithium ion transference number is <0.5 [25–27]. However, for SPE application in lithium power sources, it is highly desirable to achieve Li^+ transference number close to unity. It may be done, for example, using special admixtures [28]. In the system studied, the total conductivity is low, and the more important task is to increase the overall conductivity.

Differential scanning calorimetry

Glass transition temperature T_g was determined by differential scanning calorimetry (DSC) using a DSC 822e (Settler-Toledo) instrument with the Star program package at the scanning rate of 5 grad/min. As an example, Fig. 2 shows a typical DSC thermogram of the SPE with 20 wt% $LiClO_4$.

As it is seen from Fig. 2, in the temperature range from −100 to 100 °C, only a second-order phase transition is observed. First-order phase transitions, namely, crystallization or melting peaks, are absent. It indicates a completely amorphous system. The same picture is observed for other compositions of SPE.

Fourier transform infrared spectroscopy

FTIR spectra of solid polymer electrolytes and corresponding PEG-DA solutions of $LiClO_4$ before polymerization were recorded at room temperature by a Perkin-Elmer Spectrum 100 device in the range of 400–4,000 cm^{-1} with a spectral resolution of 0.5 cm^{-1}.

Quantum-chemical calculation

Quantum-chemical calculations of models of polymer chains and their complexes with Li^+ and ClO_4^- were carried out using the nonempirical PBE density functional method [29] and the extended basis set: H [6s2p/2s1p], C, O

Table 1 The dependence of σ_{sp} of PEG-DA–$LiClO_4$ on $LiClO_4$ content

σ_{sp} ($S\times cm^{-1}$) at the T (°C)	[$LiClO_4$] (wt%)			
	10	15	20	25
20	8.1×10^{-8}	1.0×10^{-7}	2.1×10^{-7}	1.9×10^{-7}
30	1.4×10^{-7}	2.0×10^{-7}	4.1×10^{-7}	3.3×10^{-7}
40	2.7×10^{-7}	4.7×10^{-7}	8.1×10^{-7}	6.7×10^{-7}
50	5.2×10^{-7}	9.0×10^{-7}	1.7×10^{-6}	1.4×10^{-6}
60	9.9×10^{-7}	1.7×10^{-6}	3.5×10^{-6}	2.8×10^{-6}
70	1.7×10^{-6}	3.4×10^{-6}	6.2×10^{-6}	4.7×10^{-6}
80	2.7×10^{-6}	5.7×10^{-6}	1.0×10^{-5}	7.5×10^{-6}
90	3.7×10^{-6}	8.5×10^{-6}	1.7×10^{-5}	1.2×10^{-5}
100	7.8×10^{-6}	1.7×10^{-5}	2.4×10^{-5}	1.6×10^{-5}

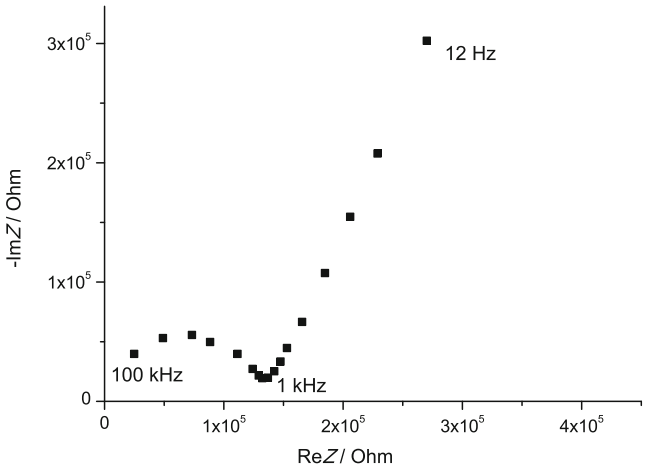

Fig. 1 The typical impedance hodograph of an electrochemical cell of SS/SPE/SS at 30 °C with SPE based on 75 wt% PEG-DA and 25 wt% $LiClO_4$

[10s7p3d/3s2p1d], and Li [10s7p3d/4s3p1d]. All calculations were performed by means of the program package PRIRODA [30] using the computational facilities of the Joint Supercomputer Center (Moscow, Russia).

Results and discussion

The samples of SPE (PEG-DA) were prepared at various concentrations of $LiClO_4$: 10, 15, 20, and 25 wt%. The results obtained are summarized in Table 2. From DSC measurements, it follows that the T_g gradually rises with increase in $LiClO_4$ content (Fig. 3), and the most considerable growth of T_g is observed in the range of $LiClO_4$ concentrations from 10 to 20 wt%. At $LiClO_4$ concentration over 20 %, the value of T_g is almost constant.

This picture of T_g changes indicates an enhancement of intermolecular bonding in the presence of $LiClO_4$. Indeed,

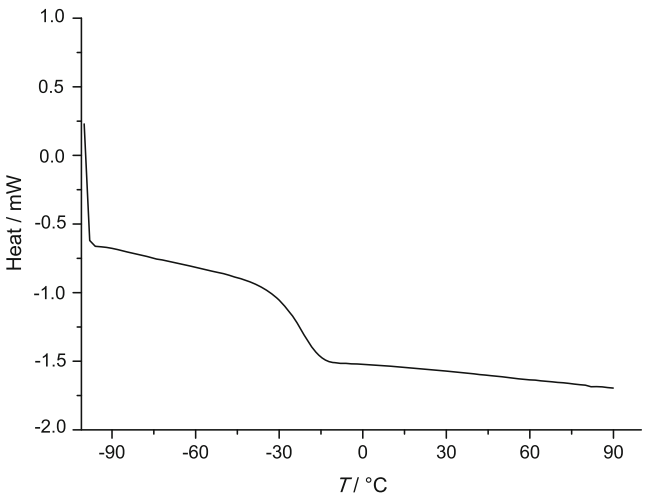

Fig. 2 DSC thermostat of the SPE with 20 wt% $LiClO_4$

the direct simulation of the polymer electrolyte structure of PEO–$LiClO_4$ by molecular dynamics at the Li–O (ether) ratio=1:7.5 [31] showed that approximately 20 % bonds of Li-PEO involve oxygen atoms belonging to different chains. Additional information is provided by study of Raman spectra of this system in the range of ν_1 vibrations of ClO_4^- anion at 25 °C. It was found the sharp change in the state of ClO_4^- anion in the system with increasing of Li–O ratio from 1:6 to 1:3, which is induced by the formation of dimers of contact ion pairs $(LiClO_4)_2$ [32]. On the basis of these data and observed dependence of T_g on [$LiClO_4$], one may assume that the appearance of glass transition temperature limit at the $LiClO_4$ content >20 wt% is caused by the saturation of the interaction between the polymer chains because of the formation of $LiClO_4$ associates.

The results of measurements of SPE specific conductivity (σ_{sp}) by electrochemical impedance spectroscopy show that the σ_{sp} achieves a maximal value of increase at $LiClO_4$ content for all samples (Fig. 4). Highest conductivity at all temperatures is achieved for the polymer electrolyte containing 20 wt% salt, which corresponds to [$LiClO_4$]=2.84 mol/dm^3.

The conductivity of the polymer electrolytes usually did not follow the Arrhenius rule, and empirical equation of Vogel–Tamman–Fulcher (FTF):

$$\sigma = AT^{-1/2}\exp(-B/T - T_0) \quad (1)$$

is often used.

In our case, it was found that Eq. (1) cannot describe the experimental data with one set of constants A and B in the whole temperature range. A similar nonlinear temperature dependence of σ_{sp} in the FTF coordinates was also observed for polymer electrolyte based on PEO monoacrylate [16]. At the same time, the temperature dependences of σ_{sp} within experimental error can be quite satisfactorily described by the Arrhenius equation over the whole temperature range. The values of the Arrhenius activation energies are given in Table 2. It is slightly varied with the salt content in the electrolyte within 12.3–13.8 kcal/mol.

Dependence of σ_{sp} on the $LiClO_4$ content has some interesting features in comparison with liquid electrolytes. As it is well known, the conductivity of liquid electrolytes also has an extreme dependence on the salt content. However, its maximum is achieved at much lower salt content of ~0.5–1 mol/l [33]. Furthermore, the conductivity of liquid electrolyte in the neighborhood of the maximum is almost constant. For the SPE considered, there is a sharp change of the ascending function σ_{sp} ([$LiClO_4$]) on the descending function σ_{sp} ([$LiClO_4$]) in the vicinity of the maximum. It is worthwhile to note that for related system based on PEG monoacrylate, a sharp maximum of conductivity was also observed, but at a lower $LiClO_4$ content of 10 wt% [16].

Table 2 Physical–chemical and spectral characteristics of SPE $(PEG\text{-}DA)_nLiClO_4$ with various $LiClO_4$ concentrations

Characteristics	$LiClO_4$ concentrations in the system of PEG-DA–$LiClO_4$ (wt%)				
	0	10	15	20	25
n	–	2.22	1.36	0.98	0.72
Li^+/O (ether)	–	1/14.4	1/8.8	1/6.3	1/4.6
Li^+/O=C–O	–	1/4.4	1/2.7	1/1.9	1/1.4
σ_{sp} (20 °C) (S×cm^{-1})	–	0.8×10^{-7}	1.0×10^{-7}	2.0×10^{-7}	1.8×10^{-7}
E_a (kcal/mol)		12.3±0.3	13.8±0.2	13.3±0.2	12.5±0.3
T_g (°C)	−30.0	−27.0	−23.4	−21.0	−20.5
The relative peak intensity at 1,649 cm^{-1}		0.09	0.09	0.09	0.13
The half-width of the peak of C–O vibrations	18	26	26	26	26

To understand the nature of these differences, the infrared spectra of the PEG-DA–$LiClO_4$ before and after polymerization were recorded, and quantum-chemical modeling was performed as well as to study intermolecular interactions of polymer-salt more detailed.

FTIR spectra of all samples are shown in Figs. 5 and 6, where the spectra presented in three specific areas: 800–1,500 cm^{-1} (Fig. 5), 1,650–1,800 cm^{-1} and 2,700–3,100 cm^{-1} for clarity (Fig. 6). The FTIR spectrum of PEG-DA is very similar to that of ethylene oxide oligomers with eight links [34].

In the 800–1,500 cm^{-1} region (Fig. 5) in the FTIR spectra of the PEG-DA samples and corresponding SPE samples, several absorption peaks are observed. These peaks correspond to the C–H deformation vibrations of CH_2 groups and the valence and deformation vibrations of C–O–C ether groups. The most intense peak of 1,109 cm^{-1} is undergoing the most significant changes at the addition of $LiClO_4$, as it was found in the case of $(PEO)_8LiClO_4$ [34].

There is overlapping of asymmetric Cl–O stretch vibration of ClO_4^- anion at 1,096 cm^{-1}, and total intensity of the absorption band of ~1,100 cm^{-1} increase with growth of $LiClO_4$ content. That is why the possible changes in the shape of the spectral lines induced by the Li^+ ions coordination on the O ether atom are masked due to the superposition of the peaks. Other bands in the range of 800–1,500 cm^{-1} are practically unchanged at $LiClO_4$ addition as for initial PEG-DA and for polymerized samples. The bands 856, 952, 1254, 1,352, and 1,453 cm^{-1} in the FTIR spectra of the SPE are present in the spectra of PEG-DA–$LiClO_4$, too. Similar absorption bands are observed in the composites of PEO/polyacrylonitrile 80/20+15 wt% $LiClO_4$ [35].

Careful analysis of the experimental IR spectra of PEG-DA–$LiClO_4$ (Fig. 5) shows that despite of the bands overlapping, the appearance of a shoulder at 1,050 cm^{-1} shifting on ~60 cm^{-1} to lower wave numbers relative to the initial peak of 1,109 cm^{-1} is seen. The intensity of the shoulder gradually increases with the concentration of Li^+ ions. It leads to a broadening of the band. For SPE, the band 1,090 cm^{-1} is more symmetrical, and its half-width is constant. The half-width is approximately the same as for the solution PEG-DA with 25 wt% $LiClO_4$. Broadening

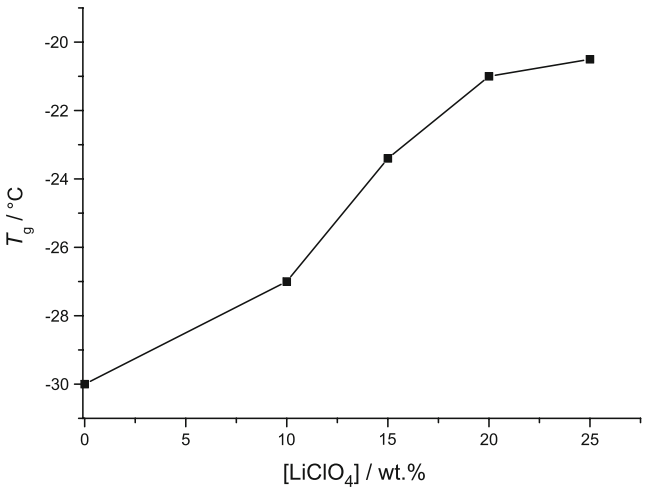

Fig. 3 The dependence of the SPE glass transition temperature on $LiClO_4$ concentration

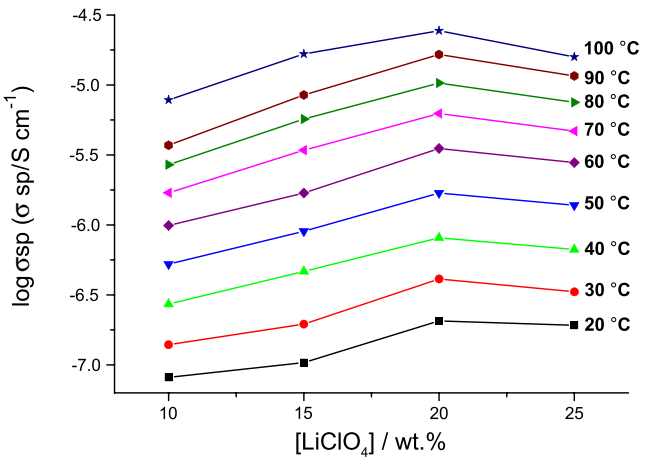

Fig. 4 Logarithmic dependence of the conductivity of SPE based on PEG-DA on $LiClO_4$ concentration at different temperatures

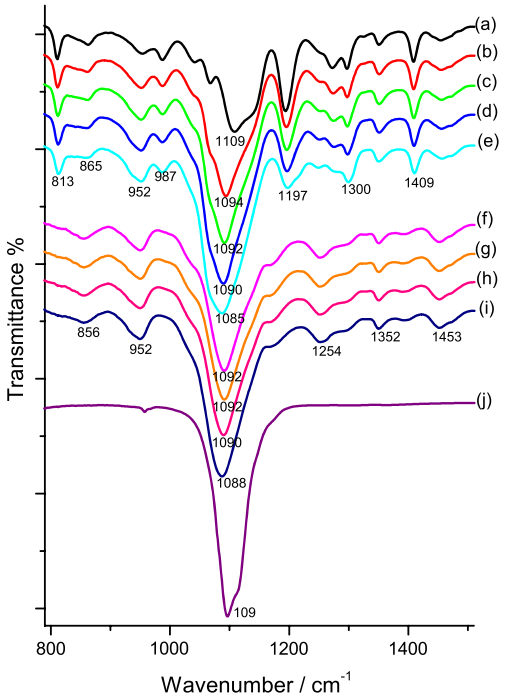

Fig. 5 The IR spectra of PEG-DA (**a**); of PEG-DA solution with different $LiClO_4$ contents (wt%): 10 (**b**), 15 (**c**), 20 (**d**), and 25 (**e**); and of SPE based on PEG-DA with different $LiClO_4$ contents (wt%): 10 (**f**), 15 (**g**), 20 (**h**), 25 (**i**), and of $LiClO_4$ (**j**)

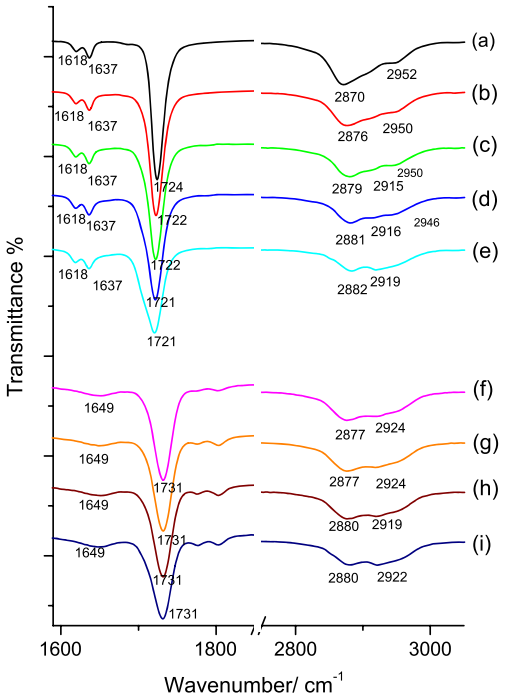

Fig. 6 The IR spectra of PEG-DA (**a**); of PEG-DA solution with different $LiClO_4$ contents (wt.%): 10 (**b**), 15 (**c**), 20 (**d**), 25 (**e**); and of SPE based on PEG-DA with different $LiClO_4$ contents (wt%): 10 (**f**), 15 (**g**), 20 (**h**), and 25 (**i**)

observed also indicates the effects of Li^+ ion coordination. Indeed, in the case of PEO–$LiClO_4$ system, the decomposition of the band of C–O–C vibrations on components demonstrates that Li^+ coordination leads to its splitting into two broad bands with peaks at 1,093 and 1,012 cm^{-1} [34].

Band of C=O vibrations of carbonyl group is located at 1,724 cm^{-1} in PEG-DA. In polymerized samples, this band is shifted to higher wave number range on 7 cm^{-1}, and doublet of C=C double bond vibrations at 1,618 and 1,637 cm^{-1} completely disappears. In the presence of $LiClO_4$, the band 1,724 cm^{-1} becomes broader and is shifted to the lower wave numbers. For the corresponding SPE, this band is located at 1,031 cm^{-1}, and its shape does not depend on the $LiClO_4$ content, and its half-width is the same as for the PEG-DA–25 wt% $LiClO_4$.

A wide band of C–H vibrations in the IR spectra of PEG-DA with a dominant peak at 2,870 cm^{-1} is broadened at addition of $LiClO_4$ salt, and its shape remains virtually unchanged during the polymerization. Figure 6 shows that the intensity of the shifted peak at 2,920 cm^{-1} increases with rising in $LiClO_4$ content.

Comparison of the observed IR spectra with those calculated for model structures will be done further.

To understand the effect of the $LiClO_4$ content on the IR spectra of the SPE obtained, the quantum-chemical study of various model structures was carried out to elucidate the interaction of Li^+ ion with polyethylene oxide units of the chain $(–CH_2CH_2O–)_n$. First of all, the structure of isolated molecules of 18-crown-6 and pentaglyme $CH_3(CH_2CH_2O)_5OCH_3$, as well as their complexes with Li^+ (see Fig. 7) were considered. It was found that the results obtained agree well with existing theoretical and experimental data.

The complex of Li^+ with 18-crown-6 has the D_{2d} symmetry. The average distance of O–Li=2.207 Å and a binding energy of Li^+ is 115 kcal/mol. The same symmetry of the most stable Li^+-18-crown-6 complex was found in B3LYP/6-31++G** study [36], the average distance of Li^+–O=2.194 Å. The six-coordinated complex of Li^+ of C_1 symmetry is higher in energy on 1.0 kcal/mol. Similar results are obtained by using extended cc-pVDZ basis set using the MP2 perturbation theory. C_1 is the ground structure in B3LYP/6-311++G** approach [37, 38], and a Li^+ binding energy is 107 kcal/mol [37]. Observed spectra of multiphoton dissociation of Li^+-18-crown-6 complex [36] have the most intensive peak at 1,075 cm^{-1} (shoulder at 1,125 cm^{-1}) and the peak at 910 cm^{-1}. The results are consistent with the existing peaks in the calculated IR spectra at 1,060, 1,100, and 910 cm^{-1} (see Fig. 8).

The most stable complex of Li^+ with pentaglyme has five Li^+–O bonds, the average distance Li^+–O=2.126 Å and binding energy is equal to 129.8 kcal/mol. Uncoordinated O atom is located at 2.726 Å distance from Li^+. The B3LYP/6-31G*//HF/3-21G* study [39] of Li^+ ion interaction with pentaglyme showed the presence of several structures with Li^+ coordination numbers 5 and 6. Energy difference

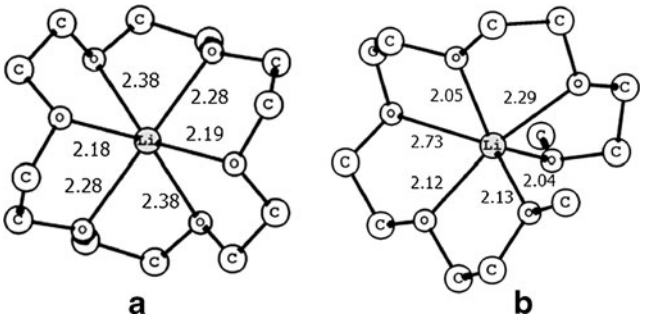

Fig. 7 The structure of the complexes of Li^+ ion with the closed (**a**) and open (**b**) cycles of polyethylene oxide units. Hydrogen atoms are omitted for clarity

between them is no more than 7 kcal/mol. B3LYP/6-31G** density functional method [40] gives that the basic structure has the coordination number 5. The average Li–O distance is equal to 2.121 Å, and Li^+ binding energy is 117.3 kcal/mol. These calculations also show the splitting of C–O vibration bands on two components, 1,136 and 1,112 cm^{-1}, at the Li^+ coordination.

Figure 8 shows the calculated IR spectra for the 18-crown-6, pentaglyme and its complexes with Li^+ in the region of 800–1,500 cm^{-1}. The most pronounced changes in the IR spectra appear in the splitting of the main peak of

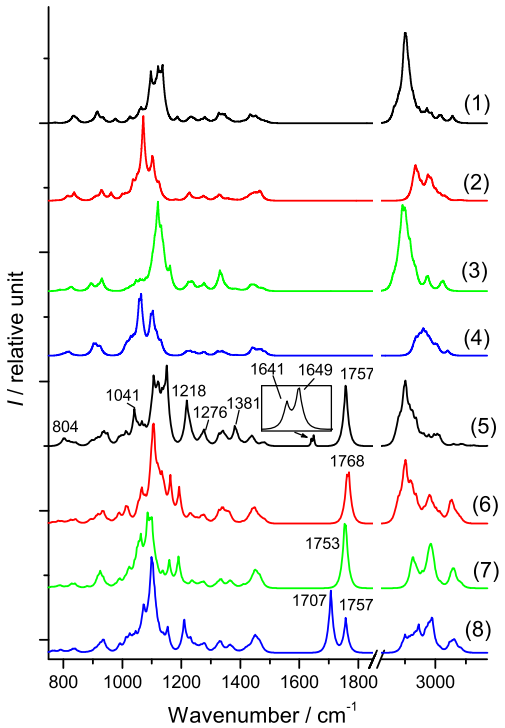

Fig. 8 Calculated IR spectra of models: *1* six units of PEO; *2* complex of Li^+ with six units of PEO; *3* 18-crown-6; *4* complex of Li^+ with 18-crown-6; *5* structure PEG-DA with C=C bonds; *6* structure PEG-DA with saturated C–C double bond; *7* structure of Li^+ complex with a fragment of the polymer chain with n=6 (structure 4 Fig. 9); *8* structure of Li^+ complex with a fragment of the polymer chain with n=6 (structure 3, Fig. 9)

C–O vibrations at ~1,100 cm^{-1} at the Li^+ coordination for both open and closed models. The new peak of C–O vibration is shifted by ~60 cm^{-1} toward lower wave numbers. The other in the region of 800–1,400 cm^{-1} has small change under Li^+ coordination. The same character of changes takes place in the experimental spectra. According to our calculations, the broadening of the peak at 1,109 cm^{-1} is associated with the appearance of the shifted C–O vibrations due to coordination of neighboring ether O atoms with Li^+ ions.

The effects of Li^+ ions coordination on O ether atoms are clearly manifested in the region of C–H vibrations (see Fig. 8). Figure 8 shows (1 and 2, 3 and 4) that the peak of C–H valence vibration at 2,900 cm^{-1} is shifted on ~60 cm^{-1} to higher wave numbers under Li^+ coordination. It indicates that the donor–acceptor electron density transfer from the ether O atoms on the Li^+ ion causes a strengthening of the C–H bonds of neighboring methylene groups. This result allows concluding that, regardless of the conformation of the PEO chain, the coordination of ether O atoms on the Li^+ ions leads to the appearance of the C–H vibrations band shifted to higher wave numbers in the IR spectrum. Just such changes are observed in the experimental spectra in the range of C–H vibrations (see Fig. 6): reduction of the main band at 2,870 cm^{-1} and increase in the intensity of the band at 2,919 cm^{-1} with rising in $LiClO_4$ concentration.

To understand features of Li^+ ions coordination in the SPE studied, the structures $CMeH_2$–$CHMeCOO(CH_2CH_2O)_n$–$OCOCHMe$–$CMeH_2$, n=5, 6 with saturated double bonds were used as model, the fragment of cross-linked polymers based on PEG-DA. The arrangement of their complexes with Li^+ and $LiClO_4$ are shown in Figs. 9 and 10, respectively. Such models are realistic from our point of view, since from molecular dynamics study of [31, 41], it follows that Li^+ ion forms predominantly a complex with a single chain of PEO. Analysis of the data allows drawing several conclusions.

Simultaneous coordination of Li^+ on two O atoms of a carbonyl group and adjacent ester group (structure 1, Fig. 9) is the most unfavorable. The reason is nonoptimal arrangement of the carbonyl group with respect to the Li^+ ion, which is seen from the elongation Li–O distance to 2.236 Å, instead of the typical values of ~2 Å in the other structures (2–4, Fig. 9). Better coordination ability of CO group results in the increase in the Li^+ binding energy to 122.4 kcal/mol in comparison with the value of 112.8 kcal/mol for the complex with pentaglyme with the same coordination number 5. Different orientation of the unbound carbonyl group (2, 3, Fig. 9) with respect to the Li^+ gives energy difference of 6 kcal/mol due to ion–dipole interactions.

In the structures considered, Li^+ has predominantly a coordination number 5. This corresponds to the results of modeling the structure of PEO–$LiClO_4$ by molecular

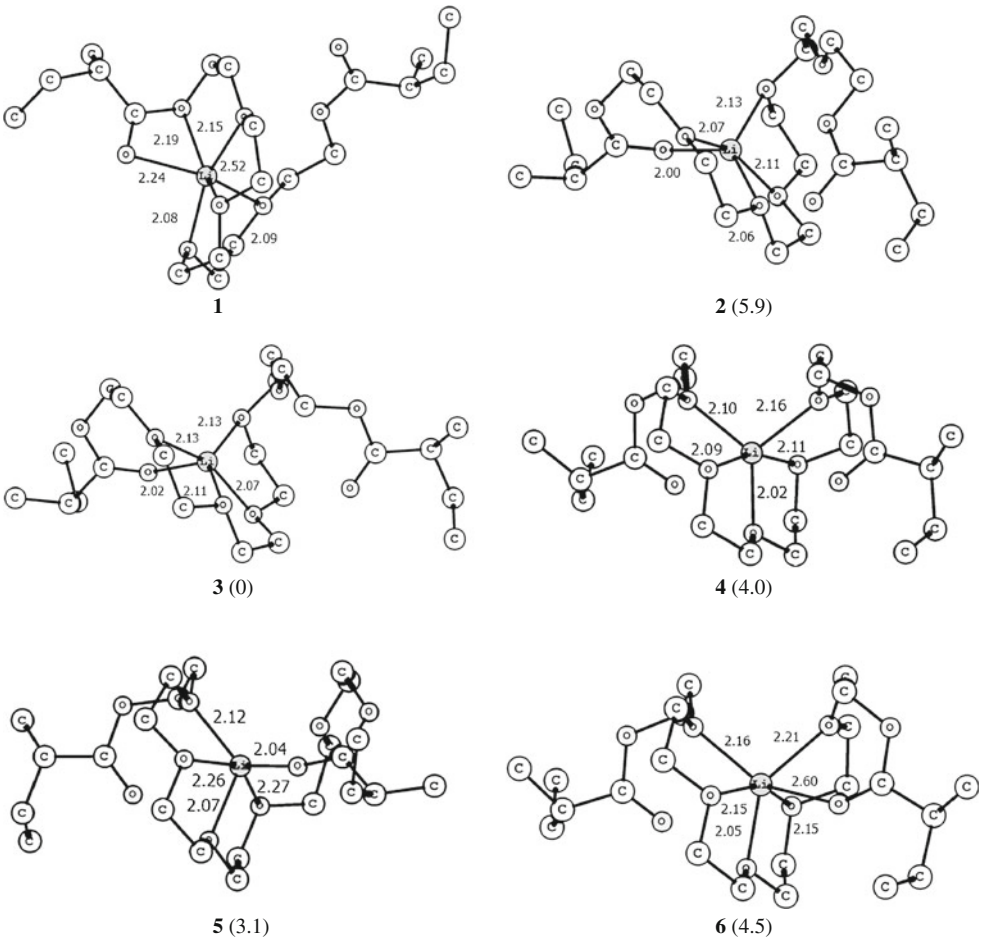

Fig. 9 Structure of Li^+ complexes with a fragment of the polymer chain with n=5 (**1**) and n=6 (**2–6**). The structure of **6** is transition state of structure transformation of **4** into the structure of **5** at Li^+ ion moving. *Figures in brackets* are the relative energies of the structures in kcal/mol. Bond lengths are in Å. Hydrogen atoms are omitted for clarity

dynamics [42] and to the experimental determination of the number of ether oxygen atoms in this system by neutron diffraction [43] as well as to the molecular structure of the crystalline phase $P(EO)_6LiClO_4$ [44].

The most noticeable difference in the IR spectra of solutions of PEG-DA–$LiClO_4$ and the corresponding polymers are the disappearance of peaks of 813, 987, 1,197, 1,300, 1,618, and 1,637 cm^{-1} and the shift of the peak of C=O vibrations on 9 cm^{-1} to higher wavenumbers (see Figs. 5 and 6).

According to the calculated the IR spectra of PEG-DA, n=6, with cis- and trans-arrangements of C=C double bonds in terminal groups and corresponding structure of $CMeH_2$–$CHMeCOO(CH_2CH_2O)_6$–$OCOCHMe$–$CMeH_2$ with saturated C=C bonds, all of these variations originated from the C=C valent vibrations or to different deformation vibrations involving the C=C fragments (see Figs. 5, 6, and 8). The last have the frequencies of 804, 1,040, 1,218, 1,276, and 1,381 cm^{-1}, which are in reliable agreement with the observations.

The calculated intensity of the trans C=C vibrations is twice higher than that for the cis C=C vibration, and their frequencies are lower than the frequency of C=O vibrations on 108 and 116 cm^{-1}, respectively. The overall intensity of the C=C vibrations is the by order of magnitude smaller than that of C=O vibrations. These theoretical data are in good agreement with the observed IR spectra.

Polymerization of PEG-DA leads to a change in environment of C=O group. This is accompanied by a high-frequency shift of the peak of C=O vibrations on 11 cm^{-1} (confer 5 and 6 in Fig. 8), which is consistent with the observed shifts of 9–10 cm^{-1} in the spectra in Fig. 6.

The Li^+ ion coordination on the PEG-DA carbonyl group causes a decrease in its frequency on 61 cm^{-1}; at the same time, the frequency of uncoordinated carbonyl group is also reduced due to Li^+ ion–C=O dipole interactions but on a smaller amount of 11–15 cm^{-1} (confer 6 and 8 in Fig. 8). In the presence of ClO_4^- counter ion in the coordination sphere of Li^+, its Coulomb field is screened. Frequency shifts of uncoordinated C=O groups are −4 and +8 cm^{-1} for structures 7 and 8 in Fig. 10, respectively. Their average is close to 0. These results allow concluding that under $LiClO_4$ dissolution in PEG-DA, the ether oxygen atoms presumably participate in the primary interaction with Li^+ ion. The observed broadening and shift of the C=O vibration band is induced by the ion–dipole interactions.

The fingerprint of C=O–Li^+ interactions is appearing in the IR spectra of SPE of a new small intensity band at 1,649 cm^{-1}, which is absent in the PEG-DA–$LiClO_4$ system. In the SPE based on monoacrylates, the broad band in the range of

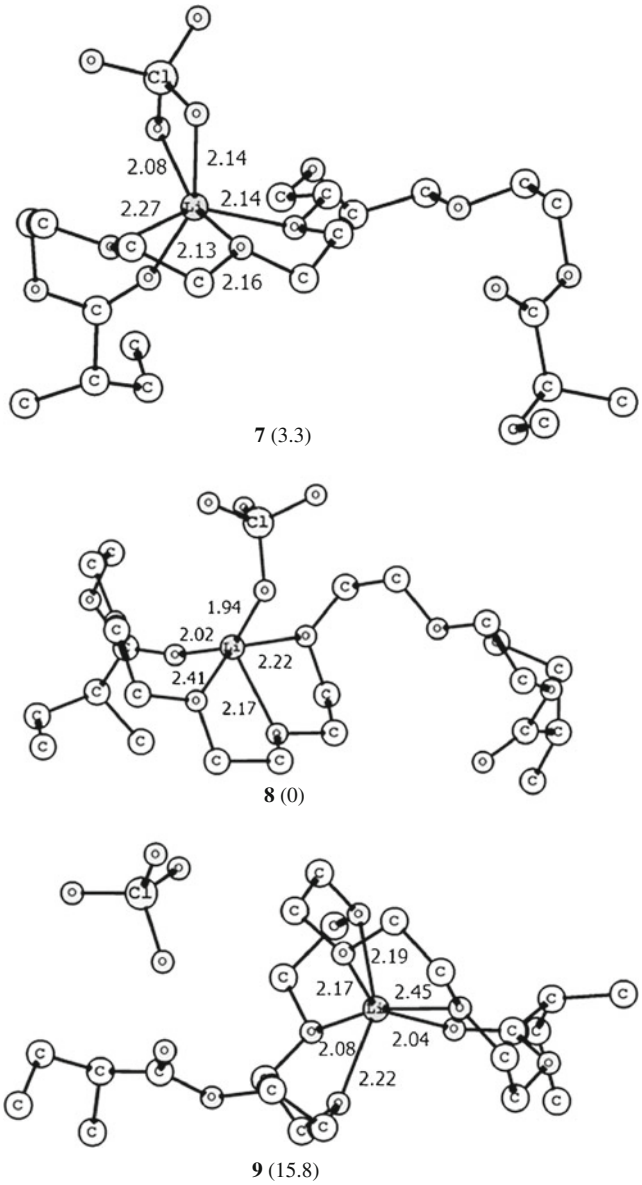

Fig. 10 Structures of the $LiClO_4$ complexes with a fragment of the polymer chains with $n=6$. The structures **7** and **8** are contact ion pair with two and one Li^+–$O(ClO_4^-)$ bonds, respectively. The structure **9** is separated ion pair. *Figures in brackets* are the relative energies of the structures in kcal/mol. Bond lengths are in Å. Hydrogen atoms are omitted for clarity

1,650 cm^{-1} is also observed, and its intensity progressively increases with $LiClO_4$ content [16]. We note that the shift of C–O vibrations band at 1,705 cm^{-1} in polyacrylates is observed at addition of $LiClO_4$ [34].

The intensity of the C=O vibrations is approximately twice increased under the Li^+ coordination. In the presence ClO_4^- this increase achieves 1.5.

The obtained vibrational characteristic of carbonyl group in the model structures is quite consistent with observed changes in the spectrum of SPE in the range of C=O vibrations. The main peak is broadened by 10 cm^{-1}, and an additional peak appears at lower wave numbers on 82 cm^{-1}.

Using the coefficient 1.5 for enhancement of intensity CO vibrations in the field of Li^+ coordinating center, one can estimate from the integrated intensities of lines in the experimental FTIR spectra that only a small part of Li^+ ions is involved in the interaction with the carbonyl groups of SPE. It decreases from 0.27 to 0.11 in the range of 10–20 wt% of $LiClO_4$ and then remains almost constant.

In cross-linked polymer, PEG-DA, all the C=O groups are in close vicinity of the main chain formed by the C–C bonds. Therefore, because of steric hindrance for optimal orientation of the C=O groups with respect to Li^+, as well as for the optimal arrangement of counter ions ClO_4^-, the probability of formation of structures with the coordination type C=O…Li^+ is reduced.

At the same time, for solutions of $LiClO_4$ in PEG-DA shifted lines of C=O vibrations, which indicate Li^+ coordination, are almost not visible. These data are in some contradiction with the results of model calculations showing that the structures with lowest energy have a carbonyl group, coordinated by the ion Li^+.

On the other hand, the structures with coordinated carbonyl group (2, 3, and 5, Fig. 9) and uncoordinated group (4, Fig. 9) have similar energy, and one can imagine that less constrains for intramolecule interaction in unpolymerized system can diminish a probability of CO…Li^+ interactions.

Besides, because of the location of the C=O group in the terminal fragment, there is the possibility of its substitution on counter ion ClO_4^- without cleavage of all other bonds of Li^+ ion with ether O atoms. In our opinion, these factor may explain the absence of fingerprints of Li^+ coordination on the C=O group in solutions.

To understand the effect of ClO_4^- counter ion on the Li^+ coordination, the complexes of $CMeH_2$–$CHMeCOO(CH_2CH_2O)_6$–$OCOCHMe$–$CMeH_2$ with $LiClO_4$ were considered (Fig. 10). The obtained values for the Li–$O(ClO_4)$ distances of 1.94, 2.08, and 2.14 Å in the contact ion pairs well agree with the shortest Li–O distances of 1.99, 2.15 in the crystal structure of $LiClO_4$ [45].

Energies of the structure with the $Li^+ClO_4^-$ contact pair (7, Fig. 10) and separated ion pair (9, Fig. 10) differ noticeably on 15.8 kcal/mol. The appearance of ClO_4^- ion in the Li^+ coordination sphere leads to an elongation of all Li–O (polymer) bonds. Formation of one or two Li^+–$O(ClO_4^-)$ bonds, see structures 7 and 8 (Fig. 10), gives little difference in energy on 3.3 kcal/mol.

At an increase in $LiClO_4$ content, the ratio Li/C=O grows up, but the part of carbonyl groups, bound to Li^+, practically is not changed. This directly indicated that additional lithium ions have another way of interaction with the polymer matrix.

The most probable reason is the growing proportion of associates of contact ion pairs Li^+ and ClO_4^-. Calculations show that $LiClO_4$ binding energy with polymer chain (structure 7) is 44.7 kcal/mol, and the calculated binding energy for $(LiClO_4)_2$ associate to the chain is 34.0 kcal/mol (corresponding structure similar to 7 is not shown). The number of bonds Li–O(polymer) is reduced to 3 in the case of Li^+ belonging to the dimer. Moreover, in the $(LiClO_4)_2$ unit, one lithium ion has unsaturated coordination and can also interact with another polymer chain. Taking into account the energy of the dimerization of $LiClO_4$ contact pairs, 41.0 kcal/mol, the formation of associates of contact pairs in the polymer matrix is energetically favorable.

The energy of transition state (structure 6, Fig. 9) of alone Li^+ ion transfer from one binding site to another is only 1 kcal/mol above the energy of equilibrium structures 4 and 5 (Fig. 9). Such type of Li^+ movements inside PEO chains are specified in the modeling of Li^+ transport in the amorphous PEO by molecular dynamics method [42]. The small activation barrier calculated is similar to that found by quantum-chemical modeling of the intermolecular hopping of lithium ion in the complex $Li^+(diglyme)_2$ [46]. Counter ion ClO_4^- forms only weak van-der-Waals bonds with polymer chains, so an activation barrier of its hopping inside polymer matrix is assumed to be also small at appropriate conformation of surrounding groups.

The situation is changed dramatically in the presence of strong Coulomb interactions between Li^+ and ClO_4^- counter ions. Then, formation of the state with separated ions (structure 9) requires large energy expenses, 15.8 kcal/mol. This value agrees qualitatively with the value of measured activation energies. Therefore, one may conclude that small conductivity of the systems is caused by very small concentration of free ions Li^+ and ClO_4^-. It should be noted that small concentration of mobile Li^+ ions in the SPE based on PEDA follows from direct determination of Li^+ self-diffusion coefficients by NMR method [21] that gives estimate of the conductivity by Nernst–Einstein equation on 2 orders of magnitude larger than the measured one.

This picture allows qualitatively to explain why equivalent conductivity (per one Li^+ ion) at 20 wt% of $LiClO_4$ is 1.5 times greater that the equivalent conductivity at 15 wt%. The reason is an increase in $LiClO_4$ dissociation degree at higher content of the salt due to energy release at interaction of a ClO_4^- ion and a contact ion pair $Li^+ClO_4^-$ with formation of complex $[Li(ClO_4)_2]^-$ ion.

The competitive process of further association of contact ion pairs becomes predominate at higher salt content 25 wt%. It is promoted by a decrease in mean distance between these pairs. As a result, the concentration of the simplest associate $Li^+ClO_4^-$, which is the main source of the mobile ions, is diminished and the conductivity of the SPE is fall down.

Conclusion

Methods of electrochemical impedance, DSC analysis, FTIR spectroscopy, and quantum chemical modeling were used to study the relationship between molecular structure and ionic conductivity of solid polymer electrolytes formed by radical polymerization of polyethylene glycol diacrylate in the presence of salt $LiClO_4$. It was found that the maximum conductivity in the range of 20–100 °C has the solid electrolyte with 20 wt% $LiClO_4$. The results of quantum chemical calculations of model complexes of Li^+ with polymer chain well correspond to the observed change in IR spectra with $LiClO_4$ content. The analysis of the data obtained indicates that Li^+ and ClO_4^- ions predominantly exist in the form of contact pairs as well as their associates in the polymer matrix. Thus, the reason for the low conductivity of the SPE studied is the small degree of dissociation of contact ion pairs. At higher $LiClO_4$ content (>20 wt%), the formation of large associates, $(LiClO_4)_3$ trimer, is accompanied by a decrease in conductivity due to lowering of contact pair content.

Acknowledgment The authors thank Dr. Baskakov S.A. for measuring of the FTIR spectra. This work was supported by the grant of the Russian Foundation for Basic Research no. 10-03-00862.

References

1. Gray FM (1997) Polymer electrolytes. The Royal Society of Chemistry, Cambridge
2. Chandrasekhar V (1998) Adv Polym Sci 135:139–205
3. Huggins RA (2009) Advanced batteries. Springer Science Business Media, New York
4. Irzhak VI, Rozenberg BA, Enikolopyan NS (1979) Network polymers: Synthesis, structure, properties. Nauka, Moscow (in Russian)
5. Hiemenz PC (1984) Polymer chemistry: the basic concepts. Basel, New York
6. Park HG, Ryu SW (2010) Polym Korea 34:357–362
7. Tang DG, Liu JH, Ci YX, Qi L (2005) Acta Phys Chim Sin 21:1263–1268
8. Kang WC, Park HG, Kim KC, Ryu SW (2009) Electrochim Acta 54:4540–4544
9. Caillon-Caravanier M, Claude-Montigny B, Lemordant D, Bosser G (2003) Solid State Ionics 156:113–127
10. Hashmi SA, Kumar A, Tripathi SK (2007) J Phys D Appl Phys 40:6527–6534
11. Vondrak J, Reiter J, Velicka J, Klapste B, Sedlarikova M, Dvorak J (2005) J Power Sources 146:436–440
12. Ramesh S, Ang GP (2010) Ionics 16:465–473
13. Reiter J, Vondrak J, Micka Z (2005) Electrochim Acta 50:4469–4476
14. Cho BW, Kim DH, Lee HW, Na BK (2007) Korean J Chem Eng 24:1037–1041
15. Lee KH, Lim HS, Wang JH (2005) J Power Sources 139:284–288
16. Zhou S, Kim D (2010) Polym Adv Technol 21:797–801
17. Lin H, Wagner EV, Swinnea JS, Freeman BD, Pas SJ, Hill AJ, Kalakkunnath S, Kalika DS (2006) J Membr Sci 276:145–161

18. Yarmolenko OV, Efimov ON, Kotova AV, Matveeva IA (2003) Russ J Electrochem 39:513–519
19. Yarmolenko OV, Baskakova YUV, Tulibaeva GZ, Bogdanova LM, Dzhavadyan EA, Komarov BA, Surkov NF, Rozenberg BA, Efimov ON (2009) Russ J Electrochem 45:101–107
20. Ishmukhametova KG, Yarmolenko OV, Bogdanova LM, Rozenberg BA, Efimov ON (2009) Russ J Electrochem 45:558–563
21. Marinin AA, Khatmullina KG, Volkov VI, Yarmolenko OV (2011) Russ J Electrochem 47:717–725
22. Khatmullina KG, Yarmolenko OV, Bogdanova LM (2010) Polym Sci Ser A Polym Phys 52:1327–1333
23. Abbrent S (2000) Lithium ion interactions in polymer gel electrolytes: effects on structure, dynamics and morthology. Doctoral thesis, Acta Universitatis Upsaliensis, Uppsala
24. Abbrent S, Lindgren J, Tegenfeldt J, Wendsjo A (1998) Electrochim Acta 43:1185–1191
25. Wang FM, Lee JT, Cheng JH, Cheng ChSh, Yang ChR (2009) J Solid State Electrochem 13:1425–1431
26. Reiche A, Tubke J, Sandner R, Werther A, Sandner B, Fleischer G (1998) Electrochim Acta 43:1429
27. Itoh T, Mitsuda Y, Ebina T, Uno T, Kubo M (2009) J Power Sources 189:531–535
28. Golodnitsky D, Kovarsky R, Mazor H, Rosenberg Y, Lapides I, Peled E, Wieczorek W, Plewa A, Siekierski M, Kalita M, Settimi L, Scrosati B, Scanlon LG (2007) J Electrochem Soc 154:A547–A553
29. Perdew P, Burke K, Ernzerhof M (1996) Phys Rev Lett 77:3865–3868
30. Laikov DN (1997) Chem Phys Lett 281:151–156
31. Siqueira LJA, Ribeiro MCC (2005) J Chem Phys 122:194911–194918
32. Ducasse L, Dussauze M, Grondin J, Lassegues JC, Naudin C, Servant L (2003) Phys Chem Chem Phys 5:567–574
33. Linden D, Reddy TB (eds) (2002) Handbook of batteries (3rd edn.) McGraw-Hill, New York
34. Dey A, Kagan S, De SK (2010) J Phys Chem Solids 71:329–335
35. Sim LH, Gan SN, Chan CH, Yahya R (2010) Spectrochim Acta Part A 76:287–292
36. Martinez-Haya B, Hurtado P, Hortal AR, Hamad S, Steill JD, Oomens J (2010) J Phys Chem A 114:7048–7054
37. Musharaf Ali S, Maity DK, De S, Shenoi MRK (2008) Desalination 232:181–190
38. De S, Boda A, Ali SM (2010) J Mol Struct (THEOCHEM) 941:90–101
39. Johansson P, Tegenfeldt J, Lindgren J (1999) Polymer 42:4399–4406
40. Dhuaml NR, Gejji SP (2006) Theor Chem Accounts 115:308–321
41. Borodin O, Smith GD (1998) Macromolecules 31:8396–8406
42. Duan Y, Halley JW, Curtiss L, Redfern P (2005) J Chem Phys 122:054702–054709
43. Mao G, Saboungi ML, Price DL, Badyal YS, Fischer HE (2001) Europhys Lett 54:347–353
44. Robitaille CD, Fauteux D (1986) J Electrochem Soc 133:315–325
45. Henderson WA, Brooks NR (2003) Inorg Chem 42:4522–4524
46. Baboul AG, Redfern PC, Sutjianto A, Curtiss LA (1999) J Am Chem Soc 121:7220–7227